THE ROLE OF MYC ACETYLATION IN BREAST CANCER

By

Emily Villalpando

A capstone project submitted for Graduation with University Honors

May 19, 2022

University Honors

University of California, Riverside

APPROVED

Dr. Ernest Martinez

Department of Biochemistry

Dr. Richard Cardullo, Howard H Hays Jr. Chair

University Honors

ABSTRACT

Overexpression of the MYC proto-oncogene has been observed in about 70% of human cancers and is associated with aggressive tumorigenesis and a poor prognosis. MYC is a transcription factor involved in several cellular processes, such as cell growth, differentiation, metabolism, proliferation, apoptosis, and gene expression. MYC is heavily regulated in physiological conditions through various mechanisms, such as its short half life and posttranslational modifications (PTMs), but has shown to be deregulated in oncogenic conditions. In cancer cells, deregulation of MYC leads to malignant transformation, but the exact pathways are yet to be completely understood. We postulate that the reliance of MYC-driven cancers on PTMs, such as acetylation of site-specific MYC lysine residues, contributes to the deregulation and overexpression of MYC in human breast cancer. In this capstone project, I discuss what is currently known in the field in regards to the role of MYC in physiological and oncogenic conditions. In addition to this, I will discuss preliminary results that aim to analyze the role of MYC acetylation in transformed human mammary epithelial cells (MCF10A). The laboratory has previously developed cell lines with lysine to arginine mutations (K149R, K158R, K323R) to inhibit lysine acetylation and determine the effects of site-specific inhibition of lysine acetylation. These results will determine the effects of these mutations on MYC protein stability and expression using cell culture and western blotting techniques. Demonstrating the role of specific acetylated lysine residues for MYC transforming activity in human cells will provide the basis for future analysis of the biological and oncogenic functions of MYC and potential clinical value of specific MYC targets for cancer therapies

ACKNOWLEDGEMENTS

I would like to thank Dr. Ernest Martinez for being a supportive, helpful mentor and for welcoming me into his laboratory during the uncertain times of COVID. A special thanks to the current and past members of the Martinez Laboratory (Jeffrey Pino, Kay Jang, Yifan Zhao, Dan-linh, and Ryan Gates) for teaching me the necessary laboratory techniques and answering all of my questions.

I am incredibly thankful to the MARC U STAR program at UCR for the support and helping me grow as a scientist, as well as for providing me with a tuition grant and stipend which allowed me to focus more on my research project.

TABLE OF CONTENTS

INTRODUCTION

Rationale

For the year of 2018, the Centers for Disease Control and Prevention reported cancer as the second leading cause of death, under heart disease, with 1 in every 4 deaths in the United States being due to cancer (U.S. Cancer Statistics Working Group, 2021). When taking a closer look at the various different types of cancers, female breast cancer was reported as having the highest rate of new diagnosed cases, leading with 254,744 new cases, and being the second highest cause of cancer death among men and women in the United States, with 42,465 breast cancer deaths in 2018 alone (U.S. Cancer Statistics Working Group, 2021).

Breast cancer is classified based on the presence or absence of three molecular markers that can be found in or on cancerous cells (Blows, 2010). The presence/absence of the estrogen receptor (ER), progesterone receptor (PR), and human epidermal growth factor receptor 2 (HER2) determine patient prognosis and suitable treatments (Blows, 2010). Based on the presence/absence of receptors, there are four molecular subtypes: luminal A, luminal B, HER2 positive, and triple negative (Fig. 1A; Engebraaten, 2013). During the years of 2015-2019, Luminal A breast cancer was the most commonly diagnosed subtype in the United States (Fig. 1B; *SEER Cancer Stat Facts: Female Breast Cancer Subtypes*, n.d.). The hormone receptor (HR) and HER2 positivity in luminal A/B and HER2 breast cancers cause a fast, uncontrollable growth of cancer cells that can be treated with specific endocrine or HER2 targeted therapies; meanwhile triple negative breast cancer (TNBC) patients have yet to have a targeted therapy for this aggressive molecular subtype (Engebraaten, 2013).

TNBC tumors tend to develop into invasive ductal carcinomas with unfavorable features, such as a larger tumor size, high grade cancer cells, and often test positive for cancer cells in the

surrounding lymph nodes (Dent, 2007). TNBC cases are often aggressive with a poor prognosis and have the lowest 5-year relative survival rate of 77.1% when comparing molecular subtypes, with the highest 5-year relative survival rate being 94.4% for HR+/HER2- cases (Fig. 1C; *SEER Cancer Stat Facts: Female Breast Cancer Subtypes*, n.d.). Comparing the patient demographic by subtype, TNBC has a disproportionately higher incidence in African American women than in non Hispanic (NH) white women, although the causes are unknown (Howlader, 2014). These disparities in breast cancer may be attributed to various differences in genetic factors and predispositions, as well as socioeconomic factors that impact people of color. This mysterious intricate interplay of biology and socioeconomic factors also lead to a lower 5-year relative survival rate of 82.2% in African American women when compared to the 91% 5-year relative survival rate of white women (U.S. Cancer Statistics Working Group, 2021).

Due to the prevalence of breast cancer cases and deaths in the United States, as well as the disproportionate impact on women of color, molecular pathways in breast cancer must be closely studied to establish molecular markers for earlier diagnosis and develop promising targeted anticancer therapies for triple negative breast cancer patients. Since triple negative cancer cells do not have the well-known targetable receptors, the Martinez Laboratory is focusing on exploring other molecular pathways implicated in tumorigenesis. The Martinez Laboratory focuses on researching the MYC proto-oncogene, specifically the lysine acetylation pathway of MYC. MYC is widely implicated in cancer due to overexpression of MYC found in about 70% of human cancers, as well as associated with aggressive tumorigenesis and a poor prognosis among patients, such as TNBC patients (Vita & Henriksson, 2006; Palaskas et al., 2011).

A

Subtypes	Hormone Receptor Status	HER2 Status	Treatments
Luminal A	ER + and/or PR +	–	Endocrine therapy
Luminal B	ER + and/or PR +	+	Endocrine therapy HER2 targeted therapy
HER2 Positive	ER – and PR –	+	HER2 targeted therapy
Triple Negative	ER – and PR –	–	Chemotherapy

B

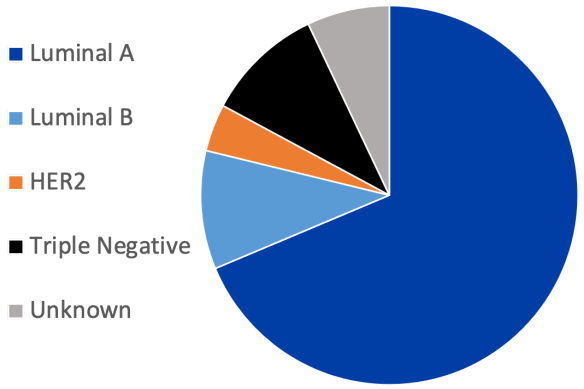

C

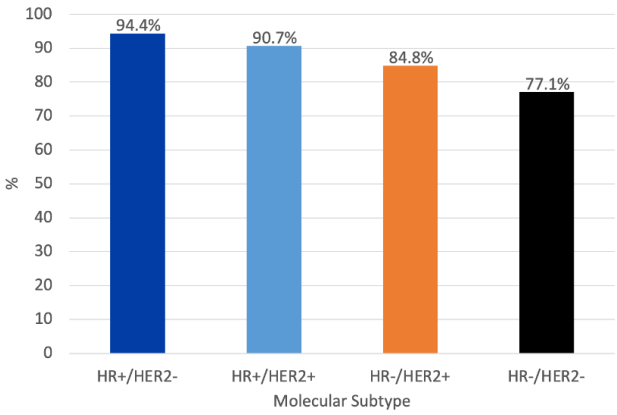

Figure 1. The Molecular Subtypes of Human Breast Cancer (A) The molecular subtypes of breast cancer, classified by hormone receptor and HER2 status. Each subtype can be treated depending on receptor status. Table information based on Engebraaten (2013). (B) Percent of female breast cancer cases by molecular subtype during the years of 2015-2019 in the United States. Data based on *SEER Cancer Stat Facts: Female Breast Cancer Subtypes* (n.d). (C) 5-Year relative survival percent of female breast cases by cancer subtype during the years of 2012-2018

in the United States. Data based on *SEER Cancer Stat Facts: Female Breast Cancer Subtypes* (n.d.)

Background

MYC is a proto-oncogenic transcription factor encoded by the MYC gene located on chromosome 8 (Dalla-Favera et al., 1982). The protein contains a transactivation domain (TAD), MYC boxes I-IV, a nuclear localization sequence, and a DNA binding domain (Fig. 2; Conacci-Sorrell et al., 2014). The TAD functions as a binding site for other proteins, such as histone acetyltransferase complexes, to regulate histone acetylation and gene transcription (Conacci-Sorrell et al., 2014). The DNA binding domain of MYC consists of a binding helix-loop-helix leucine zipper (bHLH LZ) motif that forms a heterodimer with the MYC-associated factor X (MAX) protein; The MYC-MAX heterodimer is essential for binding to DNA at enhancer box sequences for gene transcription activation (Fig. 3; Nair & Burley, 2003). MYC is responsible for regulating about 15% of genes in the human genome (Dang et al., 2006). Various cellular processes are regulated by MYC, such as cell growth, metabolism, cell cycle progression, proliferation, differentiation, and apoptosis (Conacci-Sorrell et al., 2014).

Under normal conditions, MYC is heavily regulated at translational and post translational levels, while also regulated by a short half life of 20-30 minutes, growth factors, and nutrients (Stine et al., 2015; Salghetti et al., 1999). When regulated, MYC allows for normal progression of the cell cycle; when deregulated, an abnormal cell cycle progression is observed due to the abundance of MYC in the cells and results in tumorigenesis (Fig. 4; Wang et al., 2021). In cancer cells, the deregulated signaling of MYC leads to the amplification and overexpression seen in cancer, although the exact mechanisms that lead to the deregulation of MYC remain relatively

unknown (Stine et al., 2015). Due to the established involvement of MYC in cancer, further investigation of MYC can provide the basis for developing a treatment suitable for difficult to treat cancers that are driven by MYC.

We, the Martinez Lab, postulate that the deregulation of post-translational chemical modifications (PTMs) of MYC influences its role in tumorigenesis. MYC is deregulated by PTMs, such as phosphorylation, ubiquitination, sumoylation and acetylation, that regulate MYC biological functions (Hann, 2006). The Martinez lab focuses on studying MYC lysine acetylation by histone acetyltransferases (HATs), which is the addition of an acetyl group to the amino head group, neutralizing the lysine side chain (Fig. 5; Rye et al., 2011). Some of the HATs that acetylate MYC are GCN5, P300, P300/CBP coactivator, and TIP60 (Faiola et al., 2005; Patel Jagruti H. et al., 2004; Vervoorts et al., 2003; Zhang et al., 2005). Acetylation of MYC can have different effects on the protein, depending on the residue acetylated or the HAT performing the acetylation, by either increasing protein stability or inducing turnover (Zhang et al., 2005).

The Martinez Laboratory and collaborators have previously identified MYC to be acetylated by p300 and GCN5 histone acetyltransferases (HATs), with their interactions being important for MYC function (Faiola et al., 2005; Zhang et al., 2005; Zhang et al., 2014). In both COS-7 and HEK293 cells, K149, K158, K317, and K323 lysine residues were determined to be major acetylation sites and contribute significantly to the net acetylation of the MYC protein (Faiola et al., 2005). Future experiments by the Martinez lab and collaborators have been based on the K149, K158, and K323 lysine residues mutated to arginine to inhibit site specific MYC acetylation to determine if lysine acetylation is deregulated in cancer cells, as well as analyze the effects of acetylation on the oncogenic transformation of cells (Hurd et al., *in preparation*).

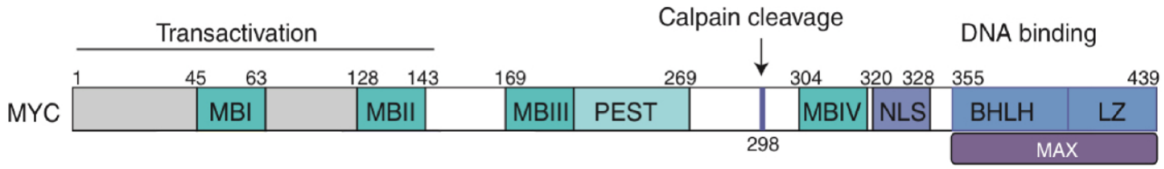

Figure 2. The Protein Organization of MYC. Image adapted from Conacci-Sorrell et al., 2014.

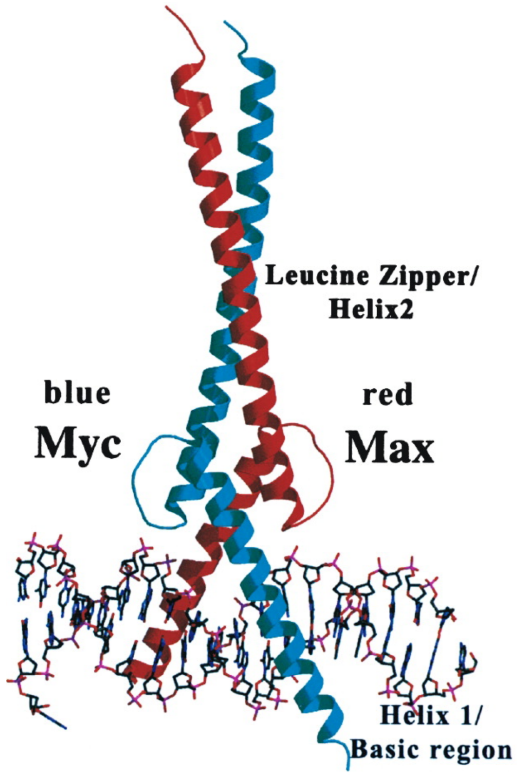

Figure 3. MYC and MAX Heterodimer Binding to DNA to Initiate Transcription of Genes. The heterodimer binds to the enhancer box motif given by the DNA sequence CACGTG (Nair & Burley, 2003). Image from Nair & Burley (2003).

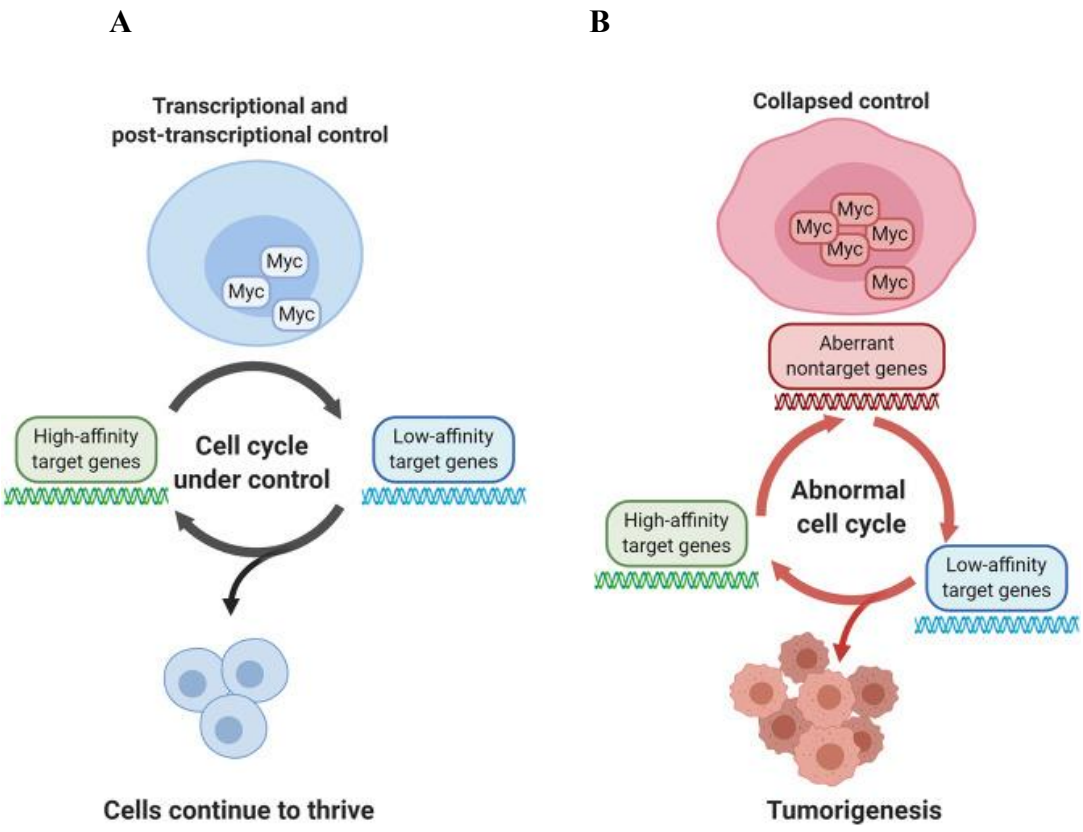

Figure 4. Representation of regulated versus deregulated MYC conditions in the human body (A) Physiological conditions of MYC. MYC is heavily regulated and the cell cycle progresses normally. (B) Deregulated MYC leads to an abnormal cell cycle progression. Image from Wang et al. (2021).

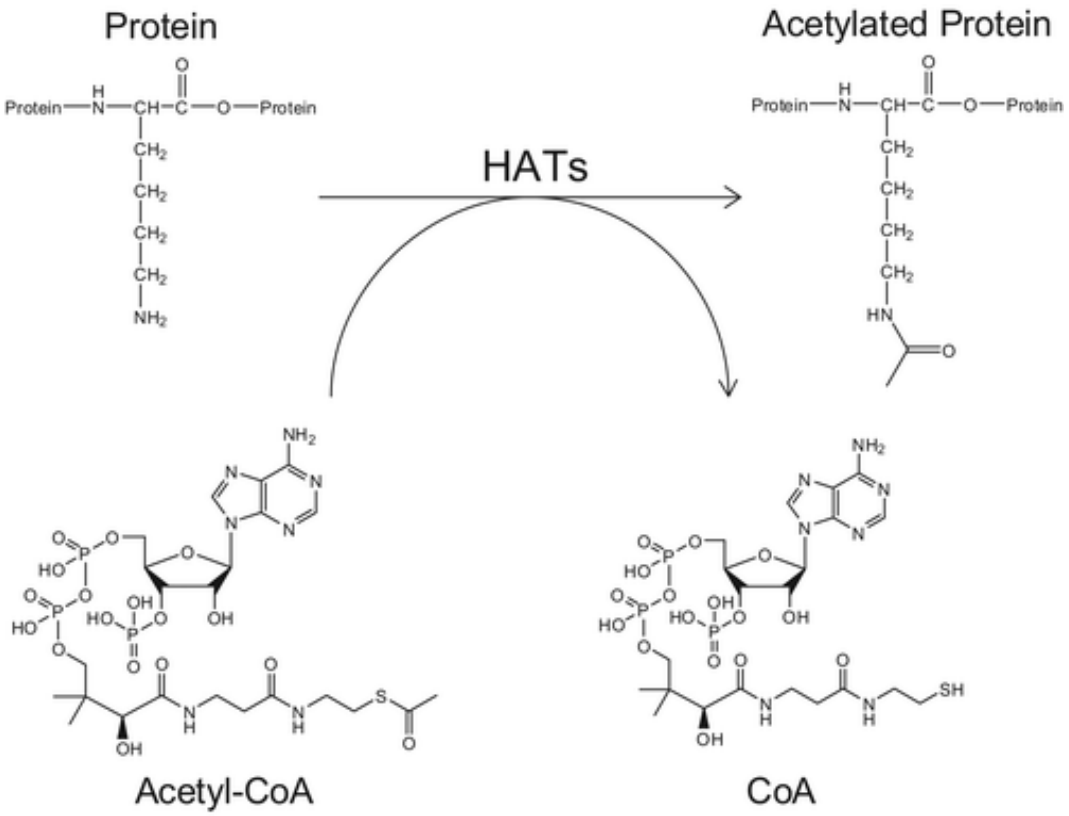

Figure 5. Representation of Lysine acetylation via interaction with HATs. Histone acetyltransferase acetylating a lysine residue, labeled as protein, by recruiting acetyl group from acetyl-CoA. Acetyl group is covalently bonded to the amide group and neutralizes the positive charge of the lysine side chain. Image from Rye et al. (2011).

Research Question

MYC is known to be deregulated in cancer cells but the exact pathways that lead to MYC overexpression are yet to be completely understood. The reliance of MYC stability on post translational modifications (PTMs), such as MYC acetylation, make PTMs a suitable target for research to determine the cause of deregulation and overexpression of MYC in human breast cancer (Faiola et al., 2005).

To address this problem, the Martinez lab studies lysine acetylation by introducing retroviral vectors that contain mouse flag-tagged MYC to MCF10A human mammary epithelial cells. Specific lysine (K) residues are mutated to arginine (R) residues to inhibit acetylation, while not affecting other MYC functions like MYC-MAX heterodimerization (Faiola et al., 2005). Lysine to arginine mutations were determined by previous experiments, as highlighted in Faiola et al. (2005), based on the lysine residues that contributed the most to the net acetylation of MYC. Experiments are conducted on 5 conditions of transduced MCF10A cells: Empty, WT, K149R, K158R, K323R. The empty vector does not contain the mouse flag-tagged MYC and will not have ectopic MYC expression, while the WT condition will express ectopic MYC, similar to MYC driven tumors. The K149R, K158R, and K323R conditions will have ectopic MYC expression and have one lysine to arginine mutation. The feasibility of mutations and the experiments conducted on MCF10A cells for this capstone are supported by results from previous experiments from the laboratory on Rat1A fibroblasts and mice that are yet to be published (Hurd et al., *in preparation*).

I aim to determine the impact, if any, of single lysine to arginine mutations of MYC on MYC protein stability and expression in MCF10A cells. To do so, I conducted a cycloheximide chase assay on MCF10A cell lines (Empty, WT, K149R, K158R, K323R), analyzed the assay via western blot, and quantified the results using ImageJ. A cycloheximide chase assay consists of exposing cells to cycloheximide, which inhibits translational elongation, resulting in the prevention of protein biosynthesis (Kao et al., 2015). This experimental technique can be used to measure protein stability of MYC because no new proteins will be made after the addition of cycloheximide and allow for the measurement of MYC degradation over time.

I expect endogenous MYC protein stability to remain similar throughout the MCF10A cell lines because the single lysine to arginine mutations introduced to the ectopic MYC should not have a large impact on total MYC in the cell. A difference in MYC protein stability should be observed when looking at the stability of flag-MYC, which considers only the ectopic MYC that was introduced into the cells. The preliminary results described in this capstone will provide a basis for determining if acetylation of K149, K158, and/or K323 residues can lead to deregulation and contribute to tumorigenesis. Overall, establishing the role of specific acetylated lysine residues in MYC transforming activity in human cells will provide the basis for future analysis of oncogenic MYC function, as well as potential clinical value of specific MYC targets for cancer therapies.

MATERIALS AND METHODS

Cell Culture

MCF10A cells were cultured in Dulbecco's Modified Eagle Medium Nutrient Mixture F-12 supplemented with 5% horse serum, 20 ng/ml epidermal growth factor (EGF), 10 μg/ml insulin, 0.5 μg/ml hydrocortisone, and 100 ng/ml cholera toxin. Recipe adapted from Debnath et al. (2003). Cells were incubated at 37°C with 5% CO_2 in 60 mm cell culture dishes. Growth medium was replaced every 2-3 days and subcultured at approximately 80-90% confluency.

Cells were maintained with a subcultivation ratio of 1:3 in accordance with the manufacturer's instructions. To subculture, the growth medium was vacuumed, then added 1 mL of 0.05% trypsin 0.5 mM EDTA and incubated for 15 minutes at 37°C with 5% CO_2. Neutralized trypsin with 2 mL of growth medium, containing trypsin inhibitors, and homogenized the mixture.

Retroviral Plasmid and Transduction

Flag-tagged mouse MYC was ligated into pMIG retroviral vector backbone (Addgene plasmid # 9044 ; http://n2t.net/addgene:9044 ; RRID:Addgene_9044). Lysine to arginine mutations in K149R, K158R, and K323R mutants were introduced via single site mutagenesis.

MYC-pMIG recombinant plasmid was introduced into 293 FT cells via transfection. After two days, the retroviral-containing medium was collected and used for transduction of MCF10A cells. The making of recombinant plasmid, transfection of 293FT cells, and transduction of MCF10A cells was performed by graduate student Jeffrey Pino in the Martinez laboratory.

Cycloheximide (CHX) Chase Assay

Plated 300,000 cells in four 60 mm plates for each cell line (E, WT, K149R, K158R, K323R), to end up with 20 plates total. Allowed for cells to form a monolayer of 90% confluency while replacing growth medium every 2-3 days, as needed.

Preparation of cycloheximide solution: 1) 20 mg of CHX per 1 ml of dimethyl sulfoxide (DMSO), 2) 240 µL of 20 mg/ml CHX to 48 mL of DMEM/F12 growth medium to achieve a concentration of 100 µg/ml CHX. Solution instructions obtained from Jeffrey Pino in the Martinez laboratory.

The 20 plates were divided into four groups and each group was exposed to CHX for a specified amount of time (t = 0, 15, 30, and 45 minutes). Each group consisted of five 60 mm plates, one plate from each cell line (E, WT, K149R, K158R, K323R). 3 mL of 100 µg/ml CHX was added to each plate in the t = 15, 30, and 45 minute groups and a timer was set for each group. Cells were lysed and collected at 0, 15, 30, and 45 minutes.

Cell Lysis

Recipe to prepare rapid protein extraction lysis buffer: 0.625 M Tris-HCl pH 6.8, 10% glycerol, 3% SDS, 0.5 mM EDTA, 5% (v/v) 2-mercaptoethanol. Recipe adapted from Silva et al. (2017).

Cells were collected at t = 0, 15, 30, and 45 minutes in the following manner. The CHX/growth medium was vacuumed and the cells were washed with 1 mL of 1X PBS. The PBS was vacuumed then 500 µL of rapid lysis buffer was added directly onto the plate. All cells were scraped from the plate using a cell scraper and pipetted into a labeled 1.5 mL eppendorf tube. Samples were placed on ice until all 20 plates were collected.

After collection, the samples were flash frozen in liquid nitrogen. Immediately after, the samples were incubated on a mixing heating block for 10 minutes at 99°C at max rpm. Samples were then flash frozen with liquid nitrogen and stored at − 80°C. Protocol for cell lysis adapted from Silva et al. (2017).

Western Blot

Sample preparation.

The protein concentration of each sample was determined via Bradford protein assay. Using the measured concentrations, the amounts required to load 80 µg of protein for the empty cell line and 100 µg for the rest (WT, K149R, K158R, K323R) were calculated. The prepared samples consisted of: the calculated amount of a sample, 6 µL of 1:1 5x SDS:1M DTT, and deionized water to end up with a total of 15µL.

SDS-Page Gel Electrophoresis.

Two 8% polyacrylamide SDS-page gels were prepared. The entire volume of each sample was loaded into a SDS-page well, along with a molecular weight marker as needed. The electrophoresis apparatus was then built and filled with 1X running buffer and ran at 160 V for approximately one hour and thirty minutes.

Transfer.

A membrane and two sponges were soaked in 1X transfer buffer, containing methanol. A "sandwich" is formed in the following sequence: sponge, gel, membrane, sponge. The "sandwich" was placed in a transfer cassette and ran for 45 minutes at a constant current of 2 V.

Blocking and Antibody Incubation.

The membrane was removed from the cassette sandwich and stained with Ponceau S for a minute to ensure transfer was successful. The membrane was washed with miliQ water and incubated in a blocking solution (6% milk solution) for 1 hour at room temperature.

Primary antibodies, MYC (Y69; Abcam) and Beta-Actin, were prepared by diluting 1:10K with 1X TBST. The membrane was incubated in primary antibody solution overnight at 4° C, constantly rocking. The next day, the membrane was washed three times with 1X TBST for 5 minutes each wash.

The secondary antibodies, rabbit and mouse, were prepared by diluting 1:10K with 1X TBST. The membrane was incubated in secondary antibody solution for 1 hour at room temperature. The membrane was then washed three times with 1X TBST for 5 minutes each wash.

Chemiluminescence.

The ECL substrate was prepared and the membrane was then incubated with ECL reagent for a 1 minute at room temperature. After, the membrane was placed in between two layers of plastic in an imaging cassette. Imaged using ChemiDoc imaging system.

Western Blot Quantification with ImageJ

The western blot was quantified using ImageJ, an image processing program developed by the National Institute of Health (Rasband, 1997). ImageJ quantifies a western blot by transforming the intensity of the bands to curves, accounting for any background; by taking the area under the curve, the intensity of a band can be represented by a number. The program can be

downloaded directly from the website <https://imagej.nih.gov/ij/index.html>, free of charge. The following highlights how to use ImageJ for quantification of a western blot, adapted from Rasband (1997):

1. Upload image of western blot
2. With your mouse, select the first band and make a rectangle that covers the entire band, as well as some of the area on top and below the band
3. Click on the top left menu: Analyze → Gels → Select first lane
    a. A number 1 should appear in the rectangular box
4. Move the rectangular box to the next band in the next lane. Analyze one set of bands at a specific molecular weight at a time
5. Click on the top left menu: Analyze → Gels → Select second lane
6. Repeat steps 4-5 as needed until all of the bands of interest are highlighted.
7. Click: Analyze → Gels → Plot Lanes
8. A graph will appear for each band previously highlighted. The curve will represent the intensity of the band, taking the background of the blot into account.
9. Take the area under the curve
    a. Select the straight line option in the ImageJ menu and make a line under each curve starting at the base of the left side of the curve to the base of the right side of the curve.
    b. Select the wand tracing tool in the ImageJ menu and select the area under the curve for each curve. ImageJ will make a spreadsheet with each area under the curve measured.
10. Repeat for each set of bands

Using the area under the curve values obtained from ImageJ, I divided each value by the area under the curve of the respective loading control (Beta-Actin) band to account for any differences in the amount of protein loaded. The values were then normalized to range from 0-1, with 1 being the amount of MYC at t = 0 minutes. The normalized values were graphed using google sheets, specifically the line chart function. Using the equation for the exponential trendline ($y = Ae^{Bt}$) given by excel, the half life of the MYC protein was calculated by solving for t and $y = 0.5$.

RESULTS

Following the Cycloheximide Chase Assay, a western blot was performed to analyze MYC protein expression (Fig. 6). The MYC (Y69) antibody used is specific to endogenous MYC, meaning the antibody detects the MYC expression originating from the cells instead of the Flag-MYC that was introduced. Observing the western blot bands by eye, a steady decrease in band intensity is observed over time with the bands at 45 minutes being the faintest. In the control (E) lanes, one band for endogenous MYC is observed for each lane (Fig. 6). The WT and mutant lanes show three bands as a result of probing with the MYC (Y69) antibody, each labeled accordingly in Figure 6. Comparing the control to the WT and mutants, the bottom band for the WT and mutant lanes must represent endogenous MYC.

The Western Blot was quantified using ImageJ, an image processing program. Using ImageJ, the intensity of the band can be represented by a curve. The area under the curve allows for quantification of the intensity of each band. Each band in Figure 6 was quantified separately according to cell line (E, WT, K149R, K158R, K323R) and molecular weight. The normalized values of the outputs from ImageJ were graphed to visualize MYC protein stability over time for each band from each cell line (Fig. 7; Fig. 8; Fig. 9). The best fit trendline was used to calculate the half life of the protein represented by a set of bands (Fig. 10). The half life of the endogenous MYC bands from E, WT, K149R, K158R, and K323R (Fig. 10) ranges from 23.86 to 46.35 minutes. The half life of the middle MYC bands from WT, K149R, K158R, and K323R (Fig. 10) ranges from 12.22 to 21.27 minutes. The half life of the top bands was not calculated due to the lack of a slope indicating degradation over the 45 minute time period.

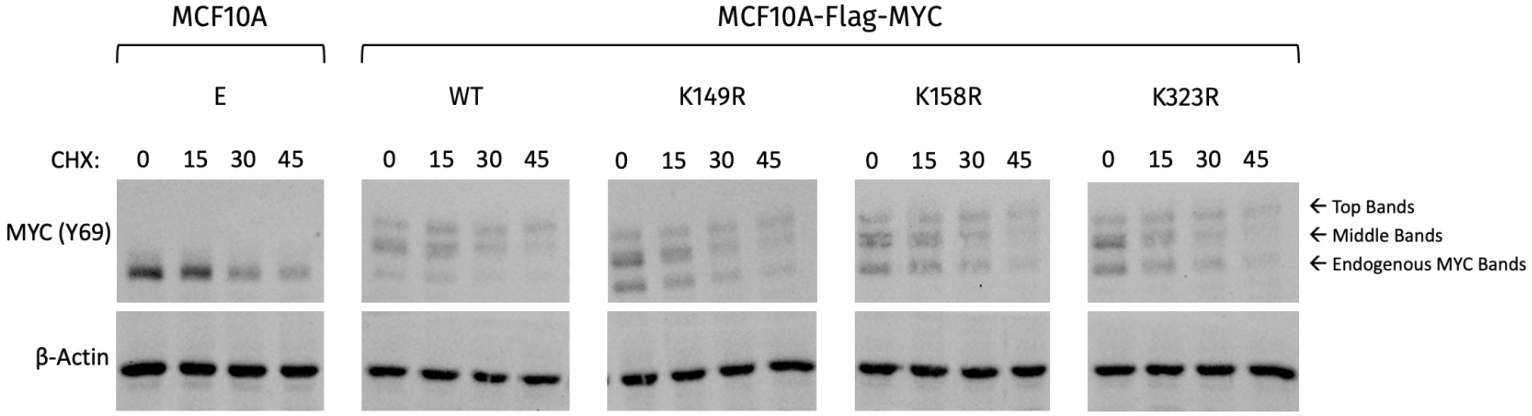

Figure 6. Western Blot Analysis of Cycloheximide Chase Assay. Western blot of whole cell extracts from MCF10A control (E), Flag-MYC WT, and K→R mutant cell lines. Each lane represents a different cycloheximide exposure ranging from 0 (no exposure) to 45 minutes. The cells were lysed and collected at their respective times then analyzed via Western Blot, probing for endogenous MYC (Y69) and using Beta-Actin as a loading control. The top portion shows bands within the 50-75 kDa range, as expected for MYC bands, and the bottom shows the loading control that falls within 37-50 kDa. Each set of MYC bands is labeled accordingly on the right.

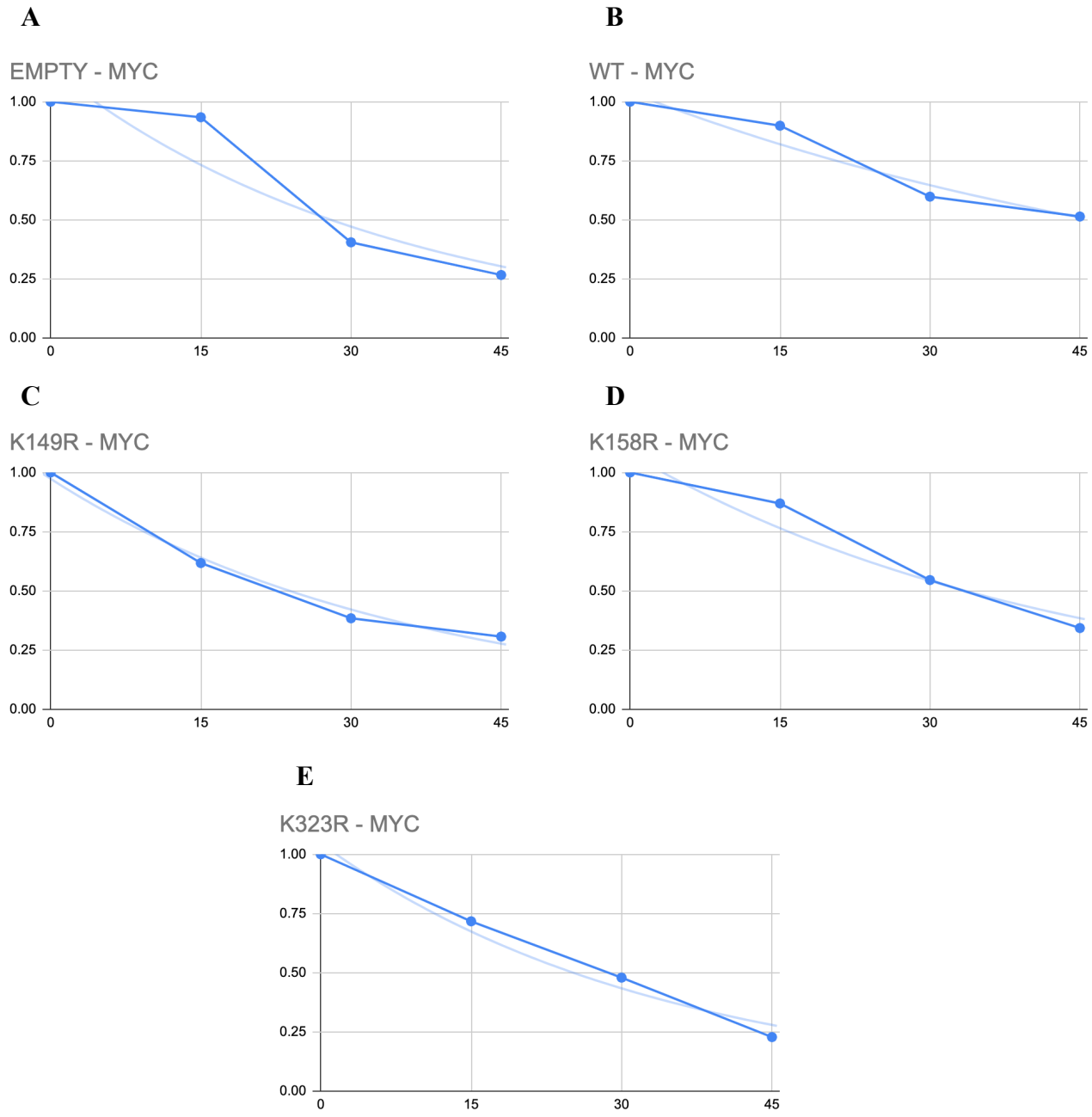

Figure 7. Normalized Curves of Endogenous MYC Band Intensities. Each graph consists of the normalized values of the intensities of each endogenous MYC band as labeled in Figure 6 (A) Normalized curve of the endogenous MYC band for the Empty group with an exponential trendline of $y = 1.14e^{-0.0294x}$ (B) Normalized curve of the endogenous MYC band for the WT group with an exponential trendline of $y = 1.04e^{-0.0158x}$ (C) Normalized curve of the

endogenous MYC band for the K149R group with an exponential trendline of $y = 0.973e^{-0.0279x}$ (D) Normalized curve of the endogenous MYC band for the K158R group with an exponential trendline of $y = 1.08e^{-0.0229x}$ (E) Normalized curve of the endogenous MYC band for the K323R group with an exponential trendline of $y = 1.05e^{-0.0293x}$

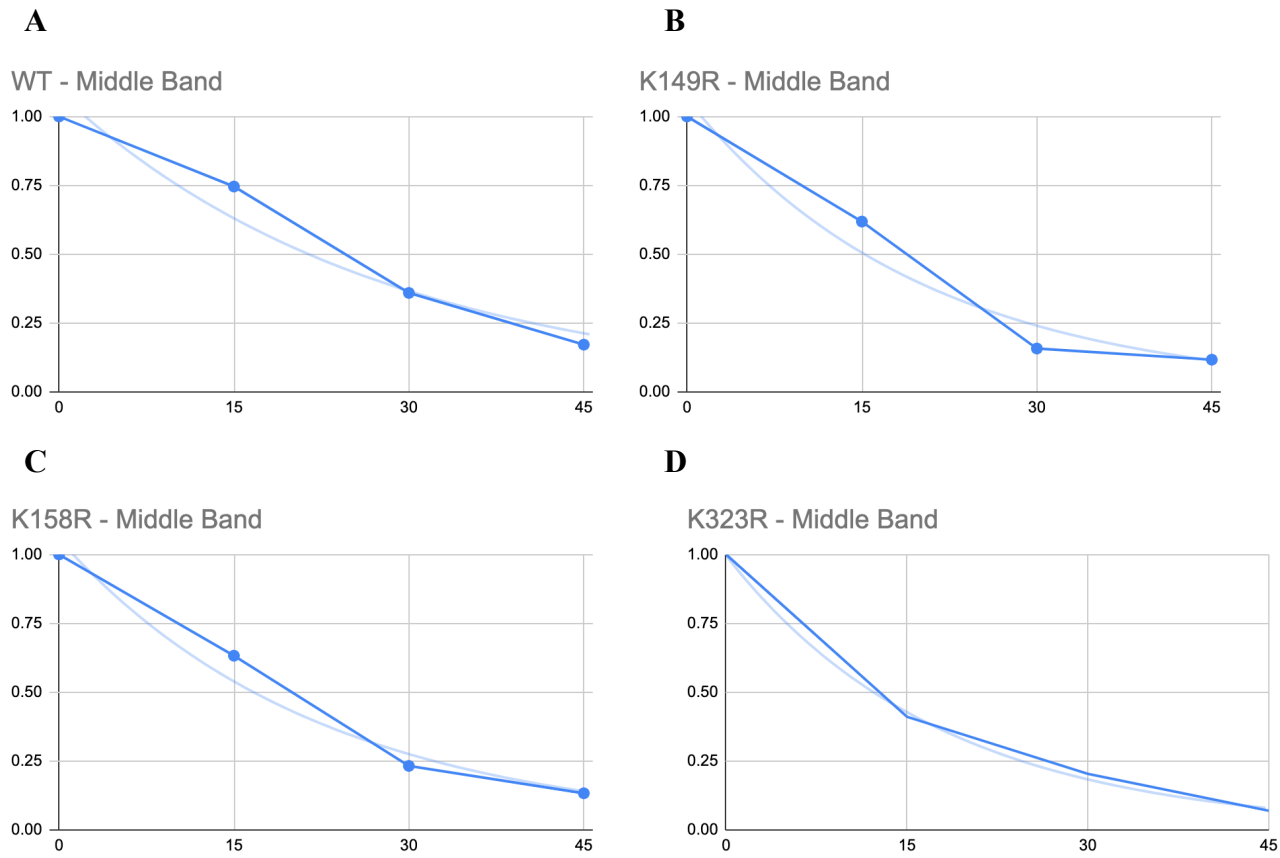

Figure 8. Normalized Curves of Middle Band Intensities. Each graph consists of the normalized values of the intensities of each middle band as labeled in Figure 6 (A) Normalized curve of the middle band for the WT group with an exponential trendline of $y = 1.08e^{-0.0362x}$ (B) Normalized curve of the middle band for the K149R group with an exponential trendline of $y = 1.06e^{-0.0495x}$ (C) Normalized curve of the middle band for the K158R group with an

exponential trendline of $y = 1.06e^{-0.0448x}$ (D) Normalized curve of the middle band for the K323R group with an exponential trendline of $y = 0.996e^{-0.0564x}$

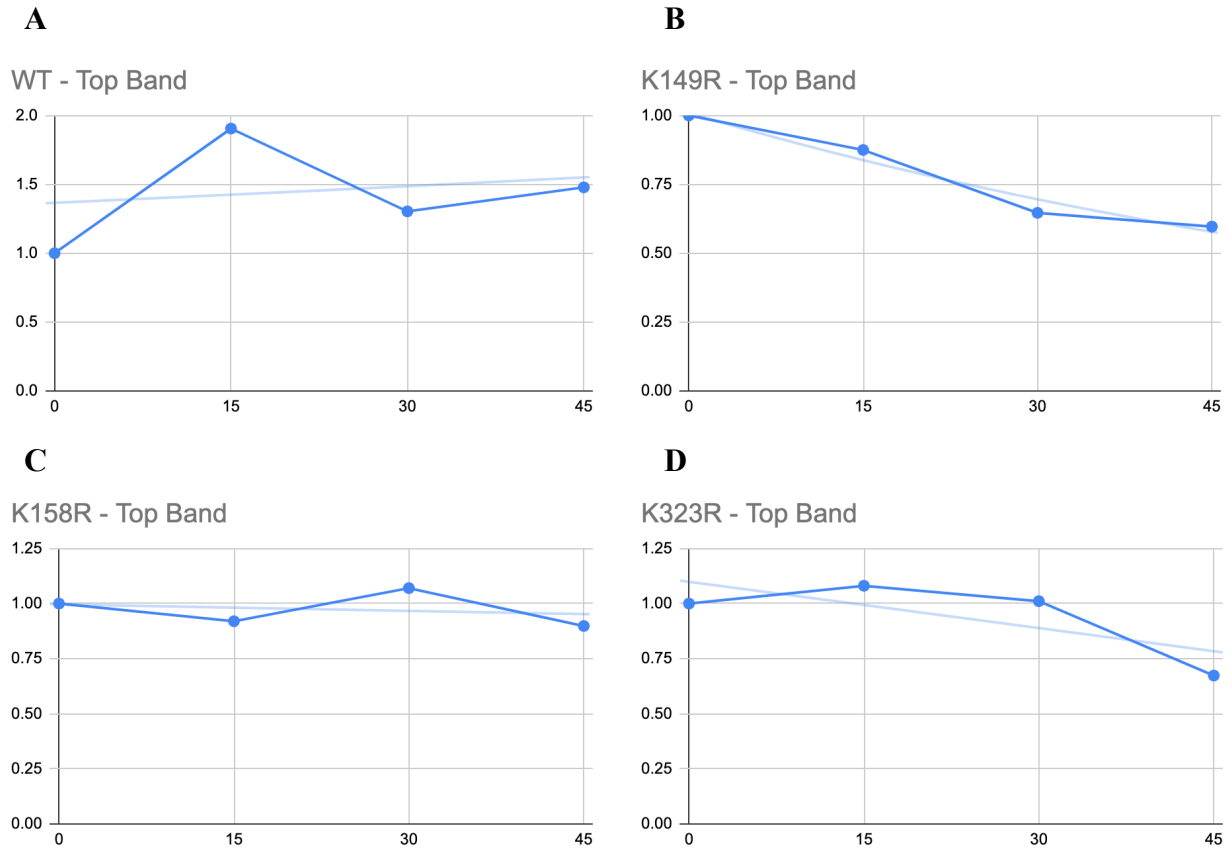

Figure 9. Normalized Curves of Top Band Intensities. Each graph consists of the normalized values of the intensities of each top band as labeled in Figure 6 (A) Normalized curve of the top bands for the WT group (B) Normalized curve of the top bands for the K149R group (C) Normalized curve of the top bands for the K158R group (D) Normalized curve of the top bands for the K323R group

Cell Line	Half Life of Endogenous MYC Band	Half Life of Middle Band
Empty	28.03	N/A
WT	46.35	21.27
K149R	23.86	15.18
K158R	33.63	16.77
K323R	25.32	12.22

Figure 10. Half Life of MYC. The values above were calculated using the trendline equations from Figures 7-9. To find the half life, let $y = 0.5$ and solve for t for any equation $y = Ae^{Bx}$

DISCUSSION AND CONCLUSION

The discovery of the MYC transcription factor was about 40 years ago, and since then MYC has become a hot topic in the world of oncology and has been mentioned in thousands of journal articles (Wasylishen & Penn, 2010). The deregulation and overexpression of MYC found in the majority and a variety of cancers makes MYC a suitable candidate for anti-cancer therapies (Vita & Henriksson, 2006). Despite the many years of research, much is still unknown about MYC, especially regarding the direct pathways that cause the deregulation of MYC. The preliminary results highlighted in this capstone aim to begin uncovering a possible pathway that leads to deregulation of MYC.

Determination of Endogenous MYC Bands

The cycloheximide chase assay conducted on MCF10A cell lines was analyzed via western blot analysis, as pictured in Figure 6. The purpose of using the MYC Y69 antibody is to determine if the individual lysine to arginine mutations have an effect on the total amount of MYC in the cell, not yet considering the ectopic MYC expression. The bands in the Empty lanes, labeled as endogenous MYC bands, at t = 0, 15, 30, 45 minutes serves as a control for the rest of the groups. No flag-tagged mouse MYC is inserted into this group and considering the MYC Y69 antibody is designed to probe for endogenous MYC, the bands shown must represent the MYC expression of "normal" human MYC. Using the Empty as a reference, I concluded that the bottom bands seen in the other lanes for the WT, K149R, K158R, and K323R groups at t = 0, 15, 30, 45 minutes must also represent endogenous MYC, as labeled in Figure 6.

Unknown Forms of MYC Detected in Western Blot Analysis

After determining the bands that represented the endogenous MYC, next came determining the two bands above the endogenous MYC band, which was only observed in the WT, K149R, K158R, and K323R groups. The WT, K149R, K158R, and K323R groups received the flag-tagged mouse MYC, either WT or mutated, which could have reacted with the MYC Y69 antibody. The middle (Fig. 8) and top bands (Fig. 9) must represent a form of MYC, since the bands appear in reaction to probing with the MYC Y69 antibody; these bands represent a heavier form considering the location of the bands on the gel in comparison to the endogenous MYC bands. The exact form of MYC that is represented by the middle (Fig. 8) and top bands (Fig. 9) is yet to be determined, as well as why two additional bands are observed in the WT, K149R, K158R, and K323R groups. The middle bands (Fig. 8) decrease in intensity over the span of 45 minutes while the top bands (Fig. 9) either do not decrease in intensity or slightly decrease. This means that the middle band (Fig. 8) represents a form of MYC that still degrades during the 45 minute period, while the top band (Fig. 9) represents a form of MYC that is highly stable when compared to the endogenous and middle MYC bands.

The Half Life of Endogenous and Ectopic MYC in MCF10A Cells

The half lives calculated for the endogenous and middle bands of the E, WT, K149R, K158R, and K323R groups are shown in Figure 10. I anticipated the half lives for endogenous MYC would be similar since I am probing for the total amount of MYC in the cells. The half lives of the observed endogenous MYC expression range from 23.86 to 46.35 minutes (Fig. 10).

The half lives of the endogenous MYC expression of the E, K149R, K158R, and K323R groups (Fig. 10) fall within the expected 20-30 minutes as reported in literature. This large range in numbers can be due to only one replicate of this experiment being analyzed at the moment. I plan to do two more replicates of this experiment to be able to take the average of the three experiments and determine if the differences in half life of endogenous MYC expression are statistically significant or not.

The half lives for the middle MYC bands of WT, K149R, K158R, and K323R cell lines (Fig. 10) range from 12.22 to 21.27 minutes, which are all values that are almost half of the endogenous MYC half lives of their respective cell line. This could mean that the middle band that represents an ectopic form of MYC also represents a less stable form since it degrades at a faster rate than endogenous MYC.

The half lives for the top bands (Fig. 9) were not calculated because there seems to be no apparent downward trend to suggest that the form of MYC represented by the top band is degrading over the span of 45 minutes. The top band represents an ectopic form of MYC, specifically a form that is observed to be significantly more stable that the other two forms in Figure 6. As of right now, it is uncertain why this form is incredibly stable but I suggest that this could be a form of ectopic MYC that contains deregulated MYC expression, considering the decrease in protein turnover that does not fall in the expected range of 20-30 minutes for MYC.

The Impact of the Lysine → Arginine Mutations on the Half Life of the MYC Protein

To better compare the half life values between the Empty, WT, K149R, K158R, and K323R groups, more replications of this experiment are necessary to use average values in a statistical analysis to determine if the difference between groups is significant or insignificant. I

would expect the differences in half life between groups to be insignificant when probing with the MYC Y69 antibody since the antibody probes for the total amount of endogenous MYC in the cell. This replicate has resulted in different half lives when comparing the Empty, WT, K149R, K158R, and K323R groups, with the half life calculated for the WT endogenous MYC expression outside of the 20-30 minute range as described in literature. A statistical analysis after obtaining multiple replicates of this experiment will determine if the differences observed in this experiment are truly significant.

REFERENCES

Blows, F. M., Driver, K. E., Schmidt, M. K., Broeks, A., van Leeuwen, F. E., Wesseling, J., Cheang, M. C., Gelmon, K., Nielsen, T. O., Blomqvist, C., Heikkilä, P., Heikkinen, T., Nevanlinna, H., Akslen, L. A., Bégin, L. R., Foulkes, W. D., Couch, F. J., Wang, X., Cafourek, V., … Huntsman, D. (2010). Subtyping of breast cancer by immunohistochemistry to investigate a relationship between subtype and short and long term survival: A collaborative analysis of data for 10,159 cases from 12 studies. *PLoS Medicine*, *7*(5), e1000279–e1000279. PubMed. https://doi.org/10.1371/journal.pmed.1000279

Conacci-Sorrell, M., McFerrin, L., & Eisenman, R. N. (2014). An overview of MYC and its interactome. *Cold Spring Harbor Perspectives in Medicine*, *4*(1), a014357–a014357. PubMed. https://doi.org/10.1101/cshperspect.a014357

Dalla-Favera, R., Bregni, M., Erikson, J., Patterson, D., Gallo, R. C., & Croce, C. M. (1982). Human c-myc onc gene is located on the region of chromosome 8 that is translocated in Burkitt lymphoma cells. *Proceedings of the National Academy of Sciences of the United States of America*, *79*(24), 7824–7827. PubMed. https://doi.org/10.1073/pnas.79.24.7824

Dang, C. V. (2012). MYC on the Path to Cancer. *Cell*, *149*(1), 22–35. https://doi.org/10.1016/j.cell.2012.03.003

Dang, C. V., O'Donnell, K. A., Zeller, K. I., Nguyen, T., Osthus, R. C., & Li, F. (2006). The c-Myc target gene network. *25 Years of the C-Myc Oncogene*, *16*(4), 253–264. https://doi.org/10.1016/j.semcancer.2006.07.014

Debnath, J., Muthuswamy, S. K., & Brugge, J. S. (2003). Morphogenesis and oncogenesis of MCF-10A mammary epithelial acini grown in three-dimensional basement membrane cultures. *Epithelial Polarity and Morphogenesis*, *30*(3), 256–268. https://doi.org/10.1016/S1046-2023(03)00032-X

Dent, R., Trudeau, M., Pritchard, K. I., Hanna, W. M., Kahn, H. K., Sawka, C. A., Lickley, L. A., Rawlinson, E., Sun, P., & Narod, S. A. (2007). Triple-Negative Breast Cancer: Clinical Features and Patterns of Recurrence. *Clinical Cancer Research*, *13*(15), 4429–4434. https://doi.org/10.1158/1078-0432.CCR-06-3045

Engebraaten, O., Vollan, H. K. M., & Børresen-Dale, A.-L. (2013). Triple-Negative Breast Cancer and the Need for New Therapeutic Targets. *The American Journal of Pathology*, *183*(4), 1064–1074. https://doi.org/10.1016/j.ajpath.2013.05.033

Faiola, F., Liu, X., Lo, S., Pan, S., Zhang, K., Lymar, E., Farina, A., & Martinez, E. (2005). Dual regulation of c-Myc by p300 via acetylation-dependent control of Myc protein turnover and coactivation of Myc-induced transcription. *Molecular and Cellular Biology*, *25*(23), 10220–10234. PubMed. https://doi.org/10.1128/MCB.25.23.10220-10234.2005

Hann, S. R. (2006). Role of post-translational modifications in regulating c-Myc proteolysis, transcriptional activity and biological function. *25 Years of the C-Myc Oncogene*, *16*(4), 288–302. https://doi.org/10.1016/j.semcancer.2006.08.004

Howlader, N., Altekruse, S. F., Li, C. I., Chen, V. W., Clarke, C. A., Ries, L. A. G., & Cronin, K. A. (2014). US Incidence of Breast Cancer Subtypes Defined by Joint Hormone Receptor and HER2 Status. *JNCI: Journal of the National Cancer Institute*, *106*(5). https://doi.org/10.1093/jnci/dju055

Kao, S.-H., Wang, W.-L., Chen, C.-Y., Chang, Y.-L., Wu, Y.-Y., Wang, Y.-T., Wang, S.-P., Nesvizhskii, A. I., Chen, Y.-J., Hong, T.-M., & Yang, P.-C. (2015). Analysis of Protein Stability by the Cycloheximide Chase Assay. *Bio-Protocol*, *5*(1), e1374. PubMed. https://doi.org/10.21769/BioProtoc.1374

Nair, S. K., & Burley, S. K. (2003). X-Ray Structures of Myc-Max and Mad-Max Recognizing DNA: Molecular Bases of Regulation by Proto-Oncogenic Transcription Factors. *Cell*, *112*(2), 193–205. https://doi.org/10.1016/S0092-8674(02)01284-9

Palaskas, N., Larson, S. M., Schultz, N., Komisopoulou, E., Wong, J., Rohle, D., Campos, C., Yannuzzi, N., Osborne, J. R., Linkov, I., Kastenhuber, E. R., Taschereau, R., Plaisier, S. B., Tran, C., Heguy, A., Wu, H., Sander, C., Phelps, M. E., Brennan, C., … Mellinghoff, I. K. (2011). 18F-fluorodeoxy-glucose positron emission tomography marks MYC-overexpressing human basal-like breast cancers. *Cancer Research*, *71*(15), 5164–5174. PubMed. https://doi.org/10.1158/0008-5472.CAN-10-4633

Parrella, P., Caballero, O. L., Sidransky, D., & Merbs, S. L. (2001). Detection of c-myc Amplification in Uveal Melanoma by Fluorescent In Situ Hybridization. *Investigative Ophthalmology & Visual Science*, *42*(8), 1679–1684.

Patel Jagruti H., Du Yanping, Ard Penny G., Phillips Charles, Carella Beth, Chen Chi-Ju, Rakowski Carrie, Chatterjee Chandrima, Lieberman Paul M., Lane William S., Blobel Gerd A., & McMahon Steven B. (2004). The c-MYC Oncoprotein Is a Substrate of the Acetyltransferases hGCN5/PCAF and TIP60. *Molecular and Cellular Biology*, *24*(24), 10826–10834. https://doi.org/10.1128/MCB.24.24.10826-10834.2004

Rasband, W. S. (1997). *ImageJ*. U. S. National Institutes of Health. https://imagej.nih.gov/ij/

Rochlitz, C. F., Heidi, I., Thiede, C., Herrmann, R., & de Kant, E. (1995). *Evidence for a mutual regulation of p53 and c-myc expression in human colorectal cancer metastases*. 981–986.

Rye, P. T., Frick, L. E., Ozbal, C. C., & Lamarr, W. A. (2011). Advances in Label-Free Screening Approaches for Studying Histone Acetyltransferases. *Journal of Biomolecular Screening*, *16*(10), 1186–1195. https://doi.org/10.1177/1087057111418653

Salghetti, S. E., Kim, S. Y., & Tansey, W. P. (1999). Destruction of Myc by ubiquitin-mediated proteolysis: Cancer-associated and transforming mutations stabilize Myc. *The EMBO Journal*, *18*(3), 717–726. PubMed. https://doi.org/10.1093/emboj/18.3.717

SEER Cancer Stat Facts: Female Breast Cancer Subtypes. (n.d.). National Cancer Institute. https://seer.cancer.gov/statfacts/html/breast-subtypes.html

Silva, R. C., Castilho, B. A., & Sattlegger, E. (2017). A Rapid Extraction Method for mammalian cell cultures, suitable for quantitative immunoblotting analysis of proteins, including phosphorylated GCN2 and eIF2α. *MethodsX*, *5*, 75–82. PubMed. https://doi.org/10.1016/j.mex.2017.10.008

Stimulation of c-MYC transcriptional activity and acetylation by recruitment of the cofactor CBP. (n.d.).

Stine, Z. E., Walton, Z. E., Altman, B. J., Hsieh, A. L., & Dang, C. V. (2015). MYC, Metabolism, and Cancer. *Cancer Discovery*, *5*(10), 1024–1039. PubMed. https://doi.org/10.1158/2159-8290.CD-15-0507

U.S. Cancer Statistics Working Group. (2021, June). *U.S. Cancer Statistics Data Visualizations Tool, based on 2020 submission data (1999–2018): U.S. Department of Health and Human Services*. Centers for Disease Control and Prevention and National Cancer Institute. www.cdc.gov/cancer/dataviz

Vita, M., & Henriksson, M. (2006). The Myc oncoprotein as a therapeutic target for human cancer. *25 Years of the C-Myc Oncogene*, *16*(4), 318–330. https://doi.org/10.1016/j.semcancer.2006.07.015

Wang, C., Zhang, J., Yin, J., Gan, Y., Xu, S., Gu, Y., & Huang, W. (2021). Alternative approaches to target Myc for cancer treatment. *Signal Transduction and Targeted Therapy*, *6*(1), 117–117. PubMed. https://doi.org/10.1038/s41392-021-00500-y

Wasylishen, A. R., & Penn, L. Z. (2010). Myc: The beauty and the beast. *Genes & Cancer*, *1*(6), 532–541. PubMed. https://doi.org/10.1177/1947601910378024

Zhang, K., Faiola, F., & Martinez, E. (2005). Six lysine residues on c-Myc are direct substrates for acetylation by p300. *Biochemical and Biophysical Research Communications*, *336*(1), 274–280. https://doi.org/10.1016/j.bbrc.2005.08.075

Zhang, N., Ichikawa, W., Faiola, F., Lo, S.-Y., Liu, X., & Martinez, E. (2014). MYC interacts with the human STAGA coactivator complex via multivalent contacts with the GCN5 and TRRAP subunits. *Biochimica et Biophysica Acta*, *1839*(5), 395–405. PubMed. https://doi.org/10.1016/j.bbagrm.2014.03.017